

The Effect of Low Temperature on the Performance of BOG Twin-Screw Compressor

Yuhang ZHOU¹, Yi GUO^{1*}, Yuli WANG², Anna DIAO², Xueyuan PENG¹

¹ Xi'an Jiaotong University, School of Energy and Power Engineering,
Xi'an, Shaanxi, China

Phone: +86 18373168010, E-mail: yiguo666@mail.xjtu.edu.cn

² Shanghai Marine Diesel Engine Research Institute,
Shanghai, China

Phone: +86 18916625493, E-mail: 18916625493@163.com

* Corresponding Author

ABSTRACT

The generation of boil-off gas (BOG) is a problem that must be solved during liquid natural gas (LNG) transportation. The dry twin-screw compressor is used for BOG recovery to ensure the purity of the gas, but the efficiency of the dry compressor is more sensitive to leakage clearance. To investigate the effect of rotor deformation on clearance and efficiency under low-temperature working conditions. This paper simulated the working process of the BOG twin-screw compressor based on the thermal-fluid-structure coupling method so that the rotor deformation could be fully considered. It found a temperature difference between the rotors, and the temperature of the male rotor was higher. Besides, when the suction temperature is -30°C, the rotors contract near the suction while expanding on the discharge side, which makes the efficiency of the compressor not significantly change. The volumetric efficiency of the operating model is 1.26% lower, while the isentropic efficiency of the operating model is 0.41% smaller than the start-up model. When the suction temperature of the compressor is -10°C, the volumetric efficiency of the compressor after stable operation increases by 3.77% compared with that at start-up, and the isentropic efficiency is increased by 5%. When the suction temperature is reduced to -50°C, the volumetric efficiency and isentropic efficiency are reduced by 9.25% and 8.25% after stable operation, respectively.

1. INTRODUCTION

Due to the change in energy structure and the shortage of fossil fuels, there is an urgent need for a green and sustainable energy substitute. Natural gas is widely used because of its low-carbon and environmentally friendly characteristics (Balcombe et al., 2021). However, the distribution of global natural gas resources is uneven, and most countries need to import natural gas. Transportation of LNG by ship is the main method of transporting natural gas. The boil-off gas (BOG) is generated due to the extremely low evaporation temperature of LNG during transportation (Migliore et al., 2017), which leads to a continuous increase in pressure in the LNG tank. It is dangerous if the pressure is not relieved in time (Noh et al., 2018). If BOG is released directly into the air, it will cause economic losses and affect the environment. The BOG recovery system is necessary in the transportation process, and the compressor is an important component of the BOG recovery system. The twin-screw compressor is used because of its compact structure, wide application range, stable operation and other advantages (Chaker et al., 2015). However, the temperature of the BOG entering the compressor is very low, and the structural thermal deformation has a deep effect on the efficiency of the screw compressor. Therefore, it is of great significance to study the variation of screw compressor performance at low temperatures.

There have been many studies about the effect of thermal deformation of parts on compressor efficiency. CFX Berlin Company calculated the temperature and pressure of the casing and rotors by the conjugated heat transfer method. The results reveal the influence of the deformation of the rotor and casing on the compressor performance (Andres et al., 2022). Saravana et al developed a conjugate heat transfer model for a screw compressor. It found that the isentropic efficiency increased by 2% compared with the model without cooling channels in the rotors (Saravana et al., 2022).

Sham et al used the bi-directional system coupling method to calculate the temperature and thermal deformation of the rotor and casing of the compressor, which provides a basis for the clearance optimization of oil-free twin-screw compressors (Rane et al., 2021). Hui Ding et al propose a fully coupled simulation approach that incorporates gas compression, conjugated heat transfer (CHT), and solid thermal expansion. It indicated that the thermal expansion of the structure affected the performance of the compressor (Ding et al., 2019).

It can be seen that in the current research, no scholars pay attention to the influence of low temperature on the performance of twin-screw compressors. Therefore, this paper adopts the thermal-fluid-structure coupling method to study the deformation of the rotors in low-temperature working conditions. The variation of compressor efficiency from start-up to operating state at different suction temperatures was analyzed.

2. SIMULATION METHOD

2.1 Geometry and Mesh

The research object of this paper is an oil-free twin-screw compressor used in a BOG recovery system. The simulation domain of the compressor includes both the fluid domain and the rotor structure, as shown in Figure 1. The blue part is the stator fluid domain, the yellow part is the rotor fluid domain, and the gray part is the male and female rotor structures. The main dimensions of the compressor include screw length, screw diameter, rotor center distance, the rotor tooth ratio, rotor warp angle and the clearance at start-up state are listed in Table 1.

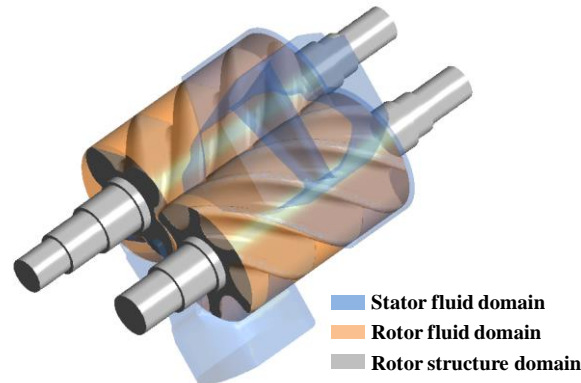


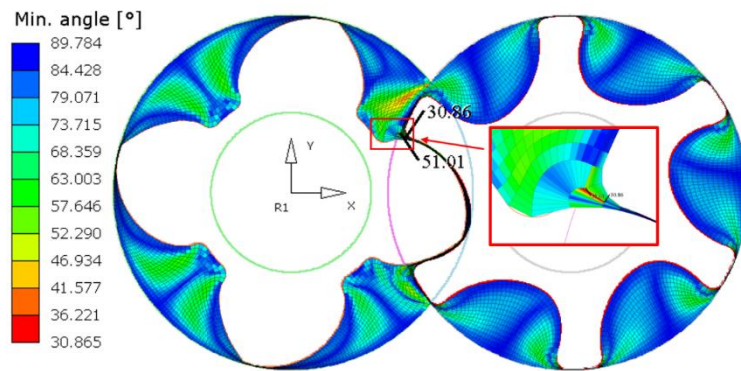
Figure 1: the fluid and structure domain of the simulation model.

Table 1: Structure parameters of the compressor

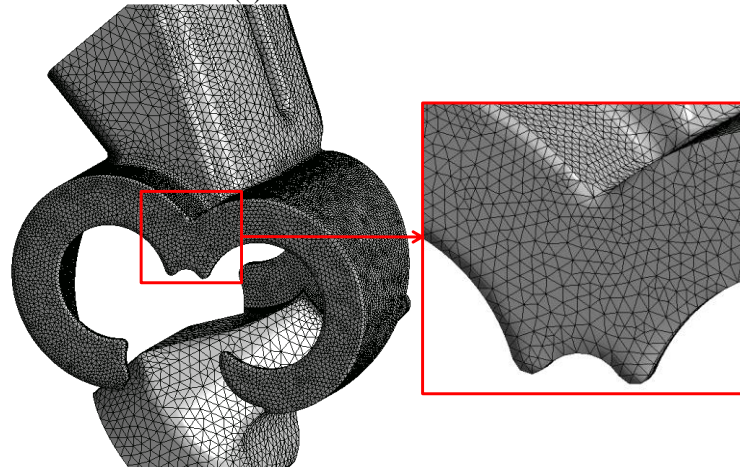
Parameter	Value
Lobe combination	4/6
Female rotor diameter/mm	178.5
Male rotor diameter/mm	178.5
Rotor length/mm	283
Center distance/mm	140
Warp angle (male rotor)/°	300
Rotor tip/mm	0.05
Meshing/mm	0.1
Suction end/mm	0.1
Discharge end/mm	0.1

For the rotor fluid domain of the compressor, the geometry is complex and changes all the time. The grid generation software TwinMesh is used to generate the grid of this part, which can eventually generate high-quality hexahedral mesh as shown in Figure 2 (a). For the stator fluid domain and rotor structure, the unstructured mesh was generated directly using the meshing module of the Ansys workbench. It can be seen from Figure 2 (b) that the mesh at the

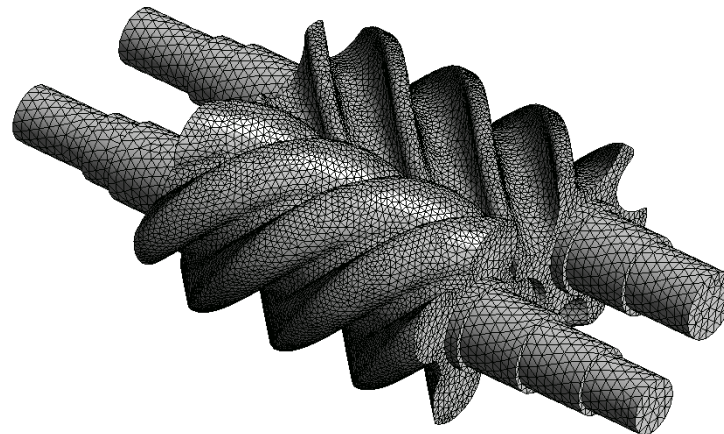
interface between the stator domain and the rotor domain is refined to ensure calculation accuracy. Figure 2 (c) shows the grid of the rotor structures.



(a) The rotor fluid domain



(b) The stator fluid domain



(c) The structure domain

Figure 2: The grid of the simulation domain

2.2 Governing Equations

The CFD simulation of a compressor is to solve the variation of thermodynamic and kinetic parameters of the mass in the flow process, which are determined by the three major conservation laws of heat transfer and fluid dynamics,

namely, conservation of mass, conservation of momentum and conservation of energy. They are expressed in the form of the equations (1)-(4).

Continuity equation:

$$\frac{\partial \rho}{\partial t} + \nabla \cdot (\rho \mathbf{U}) = 0 \quad (1)$$

Momentum conservation equation:

$$\frac{\partial(\rho \mathbf{U})}{\partial t} + \nabla \cdot (\rho \mathbf{U} \otimes \mathbf{U}) = -\nabla p + \nabla \cdot \boldsymbol{\tau} + \mathbf{F} \quad (2)$$

$$\boldsymbol{\tau} = \mu \cdot \left(\nabla \mathbf{U} + \nabla \mathbf{U}^T - \frac{2}{3} \nabla \mathbf{U} \right) \quad (3)$$

Energy conservation equation:

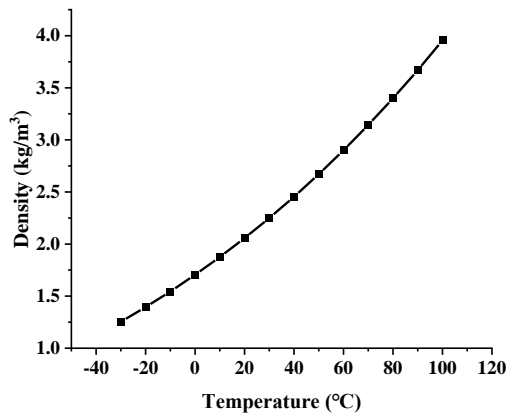
$$\frac{\partial(\rho T)}{\partial t} + \nabla \cdot (\rho \mathbf{U} T) = \nabla \cdot \left(\frac{k}{C_p} \text{grad} T \right) + S_T \quad (4)$$

where S_T is the viscous dissipative.

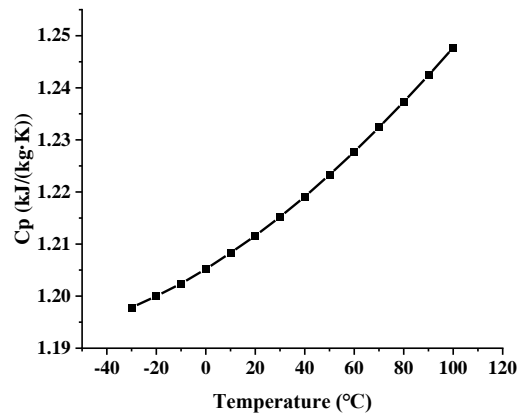
The working gas is BOG, and the main component is CH₄, mixed with a small amount of C₂H₆. Due to the dry gas seal at the shaft seal, there is high-pressure N₂, and inevitably N₂ will be mixed into the working gas. The composition is shown in Table 2. The compressibility factor of the actual gas model of the BOG in the range of operating conditions has been calculated. The result shows that the compressibility factor is close to 1 in the range of working conditions, so it is reasonable to adopt the ideal gas model. The fluid properties at the same entropy of 6.75 kJ/(kg·K) were calculated and showed in the Figure 3.

Table 2: The mass fraction of working gas

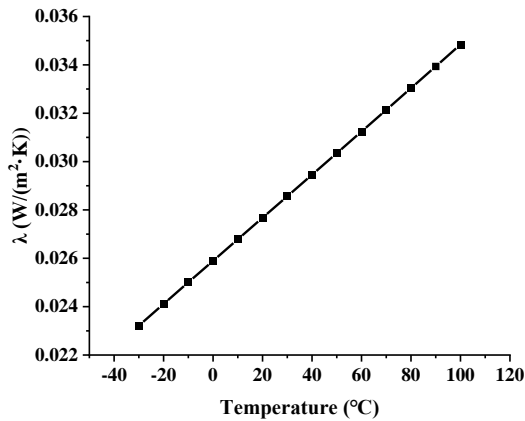
Working gas	Mass fraction/%
Methane	85.727
Nitrogen	14.255
Ethane	0.018



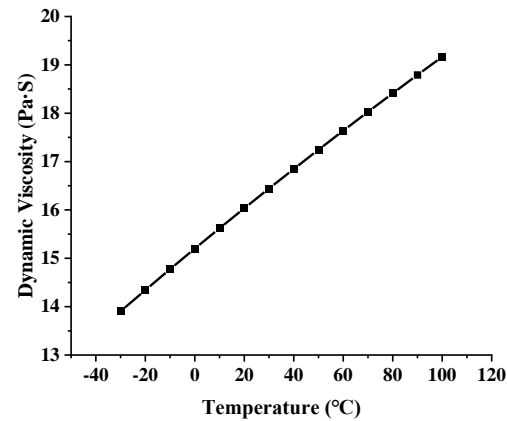
(a) The density



(b) The specific heat capacity



(c) The thermal conductivity



(d) The dynamic viscosity

Figure 3: The fluid properties at different temperatures.

In the working process of the compressor, the flow rate of the working medium is very high and is in a turbulent state, so the system also needs to introduce a turbulent transport equation. The turbulence model adopted in this paper is the SST-k- ω model, and the expression is shown in the equation (5) and (6).

$$\frac{\partial(\rho k)}{\partial t} + \frac{\partial}{\partial x_i}(\rho V_i k) = \frac{\partial}{\partial x_j} \left[\left(\mu + \frac{\mu_t}{\sigma_k} \right) \frac{\partial k}{\partial x_j} \right] + P_k - \beta \rho k \omega \quad (5)$$

$$\frac{\partial(\rho \omega)}{\partial t} + \frac{\partial}{\partial x_i}(\rho V_i \omega) = \frac{\partial}{\partial x_j} \left[\left(\mu + \frac{\mu_t}{\sigma_\omega} \right) \frac{\partial \omega}{\partial x_j} \right] + \alpha \frac{\omega}{k} P_k - \beta \rho \omega^2 \quad (6)$$

2.3 Boundary Condition

The research object of this paper is the first-stage compressor in the BOG recovery compressor unit, so the suction temperature of the compressor is low. Due to part of the cold capacity of BOG has been consumed before entering the compressor, the temperature is higher than the evaporation temperature of LNG. In this paper, the suction temperature is set at -30°C and the suction pressure is 100kPa, and the discharge pressure is 380kPa. There is cooling water flowing through the compressor casing, so the wall of the fluid domain is set as the convection heat transfer boundary. The equivalent convective heat transfer coefficient is set to 750 W·m⁻²·K⁻¹, and the cooling water temperature is set to 38°C.

Table 3: Boundary conditions of the compressor

Item	Value
Inlet Pressure/kPa	100
Inlet Temperature/°C	-30
Outlet Pressure/kPa	380
Heat Transfer Coefficient for Cooling Water/ W·m ⁻² ·K ⁻¹	750
Temperature for Cooling Water/°C	38

2.4 Simulation Method

To realize the thermal-fluid-solid coupling method, the heat transfer and deformation between fluid-solid are calculated by indirect method. The CHT method is used to insert the structure into the fluid model to realize the heat transfer between the fluid and the solid. The rotor temperature obtained is not simply the result of heat transfer to the rotor at a certain instantaneous temperature of the flow field, but the rotor finally achieves stability after many cycles of motion and heat transfer in the fluid.

- 1) The thermal performance parameters of the start-up model were calculated. The temperature of the rotor could be obtained by the CHT method.
- 2) The obtained rotor temperature is used as the boundary condition to calculate the rotor thermal deformation, and the calculated results are imported into TwinMesh to update the mesh of the rotor fluid domain.
- 3) The updated mesh is used for CFD calculation again, and the obtained thermal performance parameters are the result of considering the rotor deformation.
- 4) Repeat steps 2 and 3 until the calculated rotor temperature and deformation are no longer changing and the calculation is considered convergent. The last calculation result is the operating state.

3. RESULTS AND DISCUSSION

3.1 The Non-uniform Distribution of the Clearance

Figure 4 shows the temperature distribution of the fluid domain. It can be seen from the contour of Figure 4 (a) that a lot of high-temperature gas is distributed on the male rotor side, indicating that the leakage gas from the meshing clearance mainly enters the male rotor cavity. It can be seen from Figure 4 (b) that even though the male and female rotor cavities merge into one chamber, the temperature in the male rotor cavity is still higher than the female rotor side, and the temperature difference exists during the compression process.

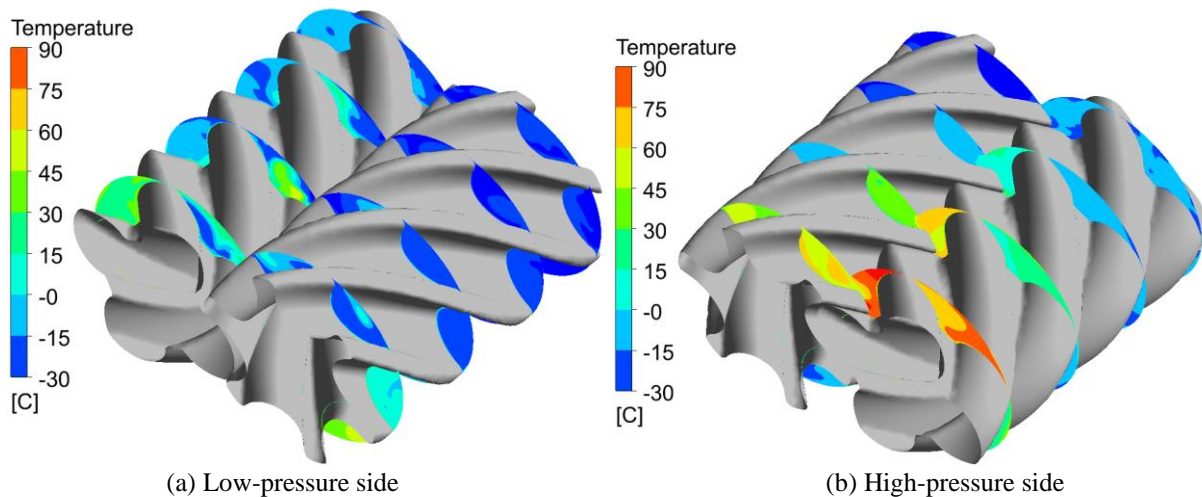


Figure 4: The temperature distribution of the fluid domain

The temperature difference of the fluid leads to the difference in the temperature of the rotor. Figure 5 shows the temperature contours of the rotors. The temperature distribution of the two rotors along the radial direction is uniform and has a linear distribution along the axial direction, which is consistent with reality. The temperature of the female rotor is lower than the male rotor, which leads to a difference in the rotor deformation.

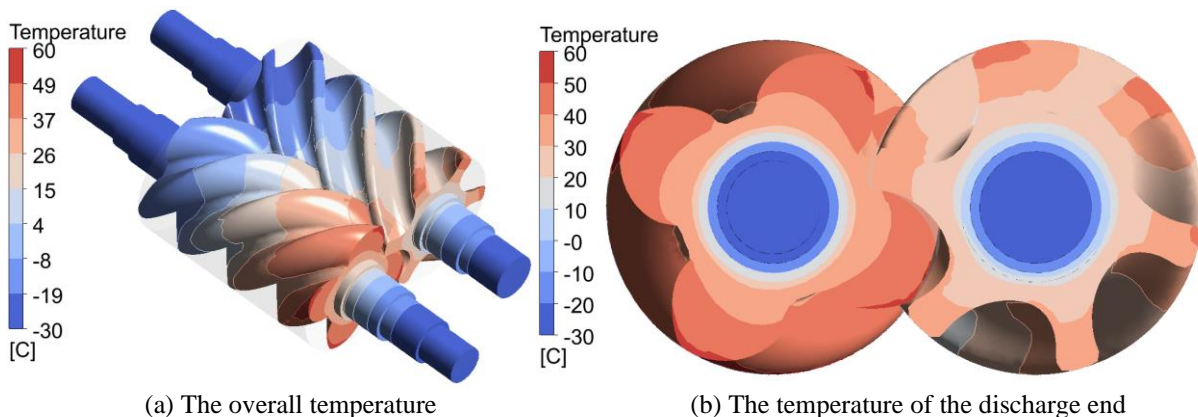


Figure 5: Temperature distribution of the rotors

Figure 6 shows the deformation of the rotors and the distribution of the clearances. The deformation shows a contract tendency near the suction end, and the contraction of the female rotor is larger. The maximum contraction of the male rotor is 0.043mm, while the female rotor is 0.05mm. The rotors show expansion at the discharge end, with a maximum value of 0.015mm for the male rotor and 0.004mm for the female rotor. The start-up tip clearance minus the deformation of the rotor is the operating tip clearance. The operating meshing clearance is simplified as the start-up meshing clearance minus the deformation of the male and female rotors. Due to the contraction of the rotors, the maximum tip clearance increased from 0.04 mm to 0.083 mm for the male rotor and 0.9 mm for the female rotor, and the maximum meshing clearance increased from 0.05 mm to 0.14 mm. The clearances decrease at the discharge side, with a minimum tip clearance of 0.035 mm for the male rotor and 0.045 mm for the female rotor, and a minimum value of 0.03 mm for the meshing clearance.

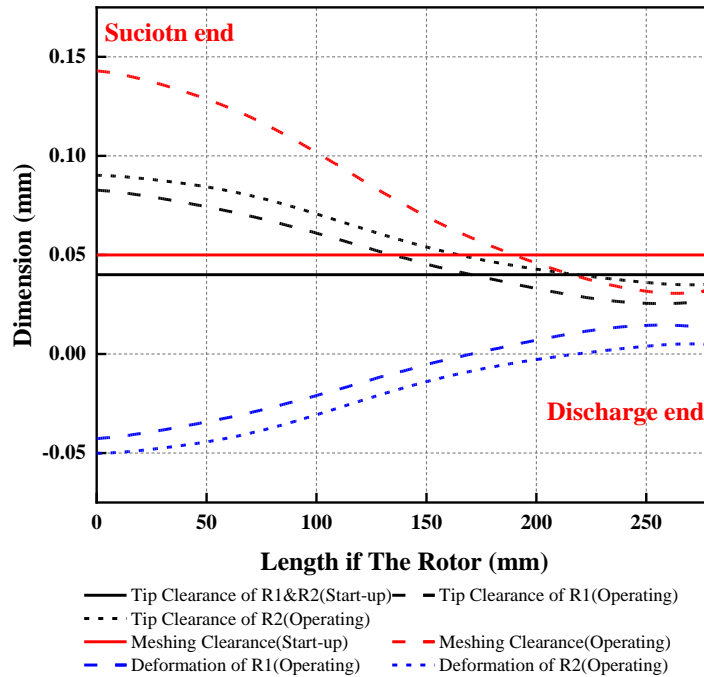


Figure 6: The rotor deformation and the clearance distribution

3.2 Influence on Compressor Efficiency

Figure 7 shows the pressure rise curves during the compression process for the two models. There is no significant difference between the two curves when the pressure is lower than 250 kPa and only a slight difference after the pressure exceeds 250 kPa. Therefore, it shows that the compression process of the compressor is hardly affected by the clearance variation. The indicated power and the isentropic power can be calculated from the pressure curve. The mass flow rate at the suction and discharge ports is also monitored and the volumetric efficiency can be calculated. The results of all calculations are shown in Table 4.

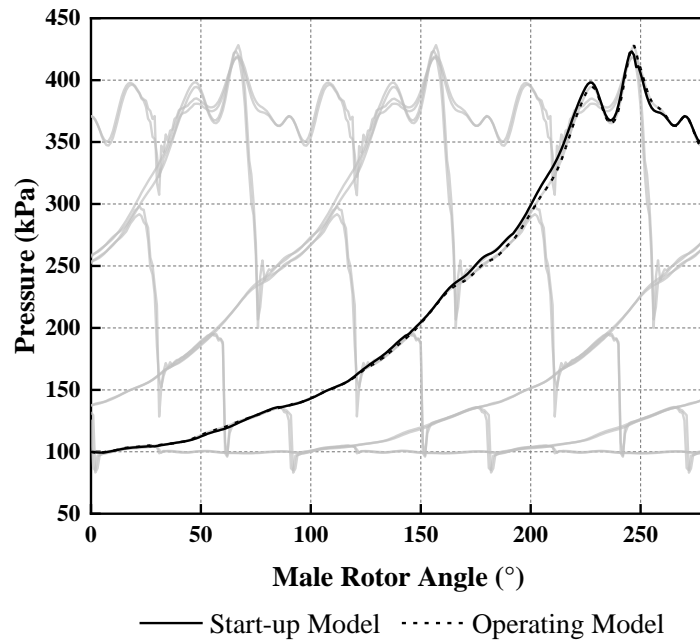


Figure 7: The p - θ diagram

Table 4: The efficiency of the three models

Model	P_{in}/kW	P_{is}/kW	$\eta_{is}/\%$	$\eta_v/\%$
Start-up	72.63	51.32	70.65	74.53
Operating	71.75	50.40	70.24	73.26

The operating model has more leakage due to the rotor deformation, which reduces the actual mass flow rate. The theoretical mass flow rate of the compressor remains the same without any change in geometry or working conditions, so the volumetric efficiency of the operating model is 1.26% lower. The indicated power of the two models is close, while the isentropic power is related to the actual mass flow rate, so the isentropic efficiency of the operating model is 0.41% smaller than the start-up model. It can be seen that there is not much difference when the suction temperature is -30°C , because although most of the clearance is increased, the clearance near the discharge end where the pressure difference is greatest is reduced, so the negative effect of low temperature on efficiency is weakened.

Therefore, to more clearly understand the effect of low-temperature intake on compressor efficiency, the compressor efficiencies at different suction temperatures are calculated, and the results are shown in Figure 8. As can be seen from the figure, when the suction temperature of the compressor is -10°C , the volumetric efficiency of the compressor after stable operation increases by 3.77% compared with that at start-up, and the isentropic efficiency is increased by 5%. When the suction temperature is reduced to -50°C , the volumetric efficiency and isentropic efficiency are reduced by 9.25% and 8.25% after stable operation, respectively.

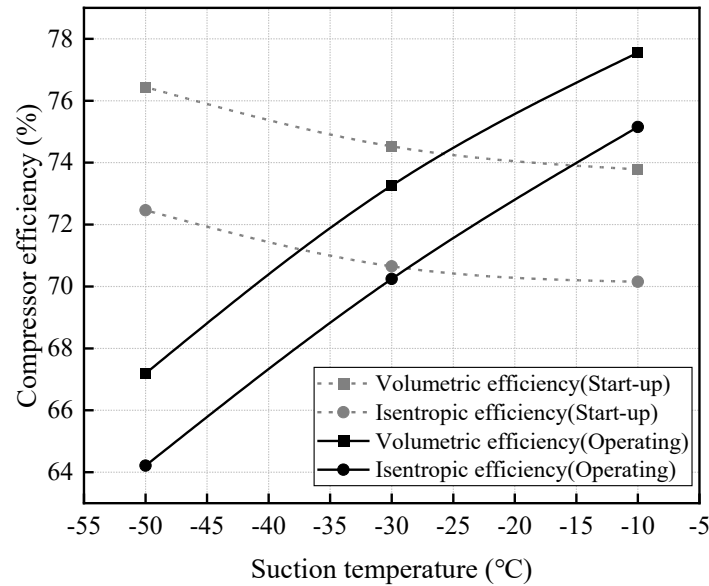


Figure 8: The compressor efficiency with the suction temperature

CONCLUSION

In this paper, the thermal-fluid-structure coupling calculation of the BOG twin-screw compressor is used to calculate the temperature distribution of the rotors, as well as the thermal deformation of the rotor. The variation and the non-uniform distribution of the clearance are obtained based on the rotor deformation. By comparing each performance parameter of the start-up model and operating model, the influence of the non-uniform distribution of the clearance on the compressor efficiency is revealed.

- 1) The leakage gas mainly flows to the male rotor side, which increases the temperature of the male rotor cavity, resulting in a higher temperature of the male rotor than the female rotor.
- 2) The change in compressor efficiency is not obvious at the suction temperature of -30°C . The volumetric efficiency of the operating model is 1.26% lower, while the isentropic efficiency of the operating model is 0.41% smaller than the start-up model.
- 3) When the suction temperature of the compressor is -10°C , the volumetric efficiency of the compressor after stable operation increases by 3.77% compared with that at start-up, and the isentropic efficiency is increased by 5%.
- 4) When the suction temperature is reduced to -50°C , the volumetric efficiency and isentropic efficiency are reduced by 9.25% and 8.25% after stable operation, respectively.

NOMENCLATURE

U	velocity	(m/s)
ρ	density	(kg/m ³)
p	pressure	(kPa)
T	temperature	(K)
k	thermal conductivity	(W·m ⁻¹ ·K ⁻¹)
μ	dynamic viscosity	(N·m/s ²)
C_p	specific heat capacity	(J·kg ⁻¹ ·K ⁻¹)
P	power	(W)
η	efficiency	(-)

Subscripts

i_s	isentropic
i_n	indicated
v	volumetric

REFERENCES

- Andres, R., Hesse, J., & Spille, A. (2022). Investigation of radial gap size change under load and the impact on performance for a twin screw compressor using numerical simulation. *IOP Conference Series: Materials Science and Engineering*, 1267(1), 012007. <https://doi.org/10.1088/1757-899x/1267/1/012007>
- Balcombe, P., Staffell, I., Kerdan, I. G., Speirs, J. F., Brandon, N. P., & Hawkes, A. D. (2021). How can LNG-fuelled ships meet decarbonisation targets? An environmental and economic analysis. *Energy*, 227, 120462. <https://doi.org/10.1016/j.energy.2021.120462>
- Chaker, M., Meher-Homji, C. B., Pillai, P., Bhattacharya, D., & Messersmith, D. (2015). Application of Boil off Gas Compressors in Liquefied Natural Gas Plants. *Journal of Engineering for Gas Turbines and Power*, 137(4). <https://doi.org/10.1115/1.4028576>
- Ding, H., Jiang, Y., & Dhar, S. (2019). CFD Modelling of Coupled Heat Transfer between Solid and Fluid in a Twin Screw Compressor. *IOP Conference Series: Materials Science and Engineering*, 604(1). <https://doi.org/10.1088/1757-899X/604/1/012005>
- Migliore, C., Salehi, A., & Vesovic, V. (2017). A non-equilibrium approach to modelling the weathering of stored Liquefied Natural Gas (LNG). *Energy*, 124, 684–692. <https://doi.org/10.1016/j.energy.2017.02.068>
- Noh, Y., Kim, J., Kim, J., & Chang, D. (2018). Economic evaluation of BOG management systems with LNG cold energy recovery in LNG import terminals considering quantitative assessment of equipment failures. *Applied Thermal Engineering*, 143(March), 1034–1045. <https://doi.org/10.1016/j.applthermaleng.2018.08.029>
- Rane, S., Kovačević, A., Stošić, N., & Smith, I. K. (2021). Bi-Directional System Coupling for Conjugate Heat Transfer and Variable Leakage Gap CFD Analysis of Twin-Screw Compressors. *IOP Conference Series: Materials Science and Engineering*, 1180(1), 012001. <https://doi.org/10.1088/1757-899x/1180/1/012001>
- Saravana, A., Liu, H., Able, N., Collins, J., Groll, E. A., & Ziviani, D. (2022). Conjugate heat transfer analysis of a twin-screw compressor with 4-6 configuration and internal cooling channels. *IOP Conference Series: Materials Science and Engineering*, 1267(1), 012014. <https://doi.org/10.1088/1757-899x/1267/1/012014>
- Wang, Z., Huang, Z., Li, T., Wang, S., Li, G., & Chen, Z. (2023). Heat transfer characteristics and deformation effects of compressor air-cooled cylinder based on heat-flow-solid coupling. *Applied Thermal Engineering*, 228(March), 120395. <https://doi.org/10.1016/j.applthermaleng.2023.120395>

ACKNOWLEDGEMENT

This work is supported by the Shanghai Marine Diesel Engine Research Institute of China (Grant No. 202106ZZ).